Proceedings of the ASME 2019 14th International Manufacturing Science and Engineering Conference MSEC 2019

June 10-14, 2019, Erie, PA, USA

MSEC2019-2896

ON THE IMPACT OF WIRELESS COMMUNICATIONS ON CONTROLLING A TWO-DIMENSIONAL GANTRY SYSTEM

Mohamed Kashef and Richard Candell*
National Institute of Standards and Technology,
Gaithersburg, Maryland
Email: {mohamed.kashef, richard.candell}@nist.gov

Sebti Foufou
University of Burgundy,
Dijon, France
Email: sfoufou@u-bourgogne.fr

ABSTRACT

Industrial wireless is essential to achieve the vision of future manufacturing systems which are highly dynamic and reconfigurable, and communicate large amounts of data. Main challenges of wireless deployment include the stochastic nature of the wireless channels and the harsh industrial transmission environment. In this work, a typical two-dimensional gantry system is controlled by a local controller which receives G-code commands wirelessly over a Wi-Fi network. The industrial wireless channel is replicated using a radio frequency (RF) channel emulator where various scenarios are considered and various wireless channel parameters are studied. The movement of the gantry system tool is tracked using a vision tracking system to quantify the impact of the wireless channel on the system performance. Numerical results are presented including the total run time of an industrial process and the dwell times at various positions through the process.

Introduction

In future manufacturing systems, wireless communications technology plays an important role in achieving flexibility and scalability through allowing the communications between larger numbers of sensors and actuators and allowing more flexible mobility of equipment. The use of wireless communications in factory automation faces various challenges including the delay and reliability requirements, and the harsh industrial radio frequency (RF) environments [1]. Most of the established industrial wireless technologies such as WirelessHART and ISA100.11a are developed for low data rate process automation applications [2]. On the other hand, home and office wireless technologies such as Bluetooth and Wi-Fi can be used for some high data rate industrial applications depending on their requirements [3].

Gantry systems are widely adopted in various industrial applications where they can be used to hold and position a variety of tools for different purposes. Examples of applications include electronic boards assembly, material handling, sorting, scanning, pick and place, welding, cutting, and plotting. Typically, the motor controller is connected using wires to the gantry system motors for path control. However, the task commands and supervisory control in a factory work-cell can be initiated from a supervisory controller which manages the work-cell process through collecting inputs from various sensors and equipment. As a result, the use of wireless communications between the supervisory controller and the gantry system controller has the following advantages. First, it allows for more efficient operation by connecting the supervisory controller to various entities wirelessly and hence better control strategies are applied [4]. The wireless connection allows for the use of the gantry system in various applications and locations in reconfigurable work-cells [5].

*Mohamed Kashef and Richard Candell have contributed equally to this work.

The use of wireless communications in controlling various gantry systems has been considered before in the literature such as in [4], [6–8]. In [6], a centralized supervisory controller is connected to multiple gantry machines over a Wi-Fi wireless network. The goal of [6] is implementing the interface between Wi-Fi and various wired protocols. In [7], the performance of a gantry system is studied where a method for testing the delay time impacts is proposed to compare various delay sources including the wireless transmissions. In [4], the control of gantry cranes for various applications is discussed where the advantages, system architecture, and challenges are considered. In [8], a pick and place robot is controlled through Zigbee wireless transmissions. All the commands are transfered to the robot controller over the wireless network.

In this work, we evaluate the performance of a two dimensional gantry system that receives commands through a Wi-Fi wireless network. The two dimensional gantry system is a commercial one which operates through G-code commands to its controller. The G-code commands are streamed using a computer to let the gantry system perform move and wait actions in a predetermined path. The commands are transmitted over a Wi-Fi, IEEE802.11n, wireless network. All the Wi-Fi transmitters and receivers are connected to an RF channel emulator to replicate the industrial channel characteristics and control various RF channel parameters. The RF channel emulator is capable of varying the wireless link distance, channel path loss exponent, the channel impulse response (CIR), and the shadowing variance. The position of the two-dimensional gantry system is recorded using a high-resolution vision tracking system. The vision system has high resolution in both distance and time and is connected to the G-code generating computer to synchronize the experiment start time.

The remainder of the paper is organized as follows. In the following section, the system model is considered where the testbed hardware and the experiment scenario are explained in detail. Then, the data collection strategy is illustrated and the performance criteria are defined. Later, the experimental results are presented and discussed. Finally, conclusions are drawn.

System Model

In this section, we introduce the experimental setup including all the hardware components and the operating conditions. We also identify the information flow through the testbed.

Testbed Architecture The testbed is composed of four main components related to the operation of the gantry system. These components are the gantry system, the Wi-Fi network, the RF channel emulator, and the supervisory computer. First, the gantry system is a commercial X-carve machine that was made initially for engraving various types of materials [9]. In our testbed, we allowed the tool to move in two directions only, with a velocity of 8000 millimeter (mm) per minute in each direction. The position resolution of the machine is around 0.1 mm. The motors of the gantry systems are controlled through a wired connection with the controller that receives G-code commands [10] through a Universal Serial Bus (USB) port. The gantry system controller has a buffer that allows it to store up to 16 G-code commands for the continuity of task execution.

Second, the supervisory computer is responsible for generating and sending the G-code commands to the gantry system controller. In this testbed, we used a generic G-code sender in order to stream the G-code commands over the wireless network. We used an Intel Bay Trail Next Unit of Computing (NUC) with Intel N2930 Celeron processor, 8 GB Random Access Memory (RAM), and 64-bit Windows 7 operating system. It has a Qualcomm Atheros AR946x wireless network adapter with two attached antennas [11].

Third, a Wi-Fi network used for wireless data transfer is composed of the supervisory computer Wi-Fi interface, a router, and a USB to Wi-Fi converter. We have used a TP-link Wi-Fi, IEEE802.11n, commercial router. The supervisory computer has its own Wi-Fi interface originally. The gantry system controller is connected to the Wi-Fi network through a USB to Wi-Fi interface. It includes two components, namely, 1) Antaira 1-port IEEE802.11b/g/n wireless serial device server [12] which converts RS232 serial data into Wi-Fi signal, and 2) an RS232 to USB conversion which is done through running a script over a computer.

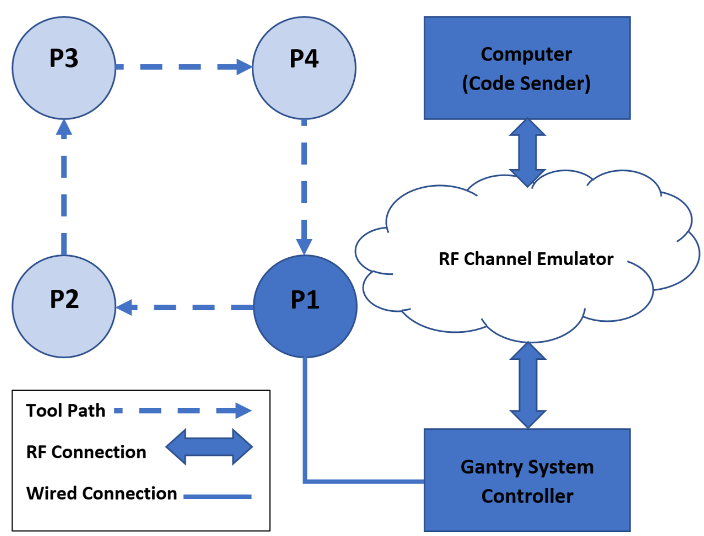

FIGURE 1. Testbed Architecture

Finally, a radio frequency channel emulator is used to replicate the multi-path and path loss environment for a mesh network of up to 8 physical nodes and 56 virtual links between those nodes. The used channel emulator is RFnest D508 and the corresponding software is RFview [13]. The channel emulator supports an instantaneous bandwidth of 250 MHz (4 nanosecond tap spacing) with an effective dynamic range of 73 dB that includes all analog and digital realization impacts. The emulator is controlled by a nearby computer which loads the path loss model and channel impulse response for each communications link.

Experimental Setup In the experimental study, we run a scenario in which the gantry tool moves sequentially between the four positions P1, P2, P3, and P4 shown in Fig. 1. The horizontal distance between P1 to P2 and P3 to P4 is 8 inches, while the vertical distance between P2 to P3 and P4 to P1 is 10 inches. The gantry system has different dwell times at each of the positions. The dwell times are 2, 1, 0.5, and 0.1 seconds for P1, P2, P3, and P4, respectively.

Each run of the above described scenario continues for 30 complete cycles over all the four positions. This scenario replicates the applications of gantry systems in various fields. It can be similar to a scenario when the gantry tool picks an item at P1 then moves it for processing at the two other positions P2 and P3. Finally, the gantry tool places the item at P4. The pick and place application can be repeated continuously over time, but we make it with a finite cycle to test various wireless channel parameters.

On the other hand, the wireless channel impact is produced through the RF channel emulator. Based on node positions, line of sight (LOS) and non-LOS (NLOS) channels may exist. LOS channels are typically characterized, compared to NLOS channels, by a lower loss exponent and a channel impulse response (CIR) with more energy on the first peak (higher K-factor). First, we consider the benchmark channel with free-space log-distance path loss and ideal CIR which has no multi-path. Second, we consider a measured delay profile of an industrial environment where the CIR is experimentally measured and processed to be deployed using the channel emulator and to reflect the industrial environment impact [1]. While deploying the measured channels, the emulator produces random Rayleigh fading channels for the NLOS cases and random Rician fading channels for the LOS cases following the injected CIRs. Moreover, time-varying log-normal shadowing is introduced due to the fluctuations in the signal level because of obstructions. The variance of zero-mean log-normal shadowing is set through the emulator.

Data Analysis

In this section, we describe the process of collecting the gantry system tool position information. Then, data processing steps are explained in detail where various performance criteria are formulated.

Data Acquisition In order to collect the position information of the gantry system tool, we used a vision tracking system. We deployed the OptiTrack V120 Trio with three cameras, frame rate of 120 frames per second, and 640 x 480 resolution per camera. The tracking system is connected to a computer for data acquisition at which the real-time position information is tracked and stored. We used the supervisory computer for controlling the vision system in order to synchronize the beginning of tracking data acquisition to the gantry system experiment start. The data acquisition setup is shown in Fig. 2.

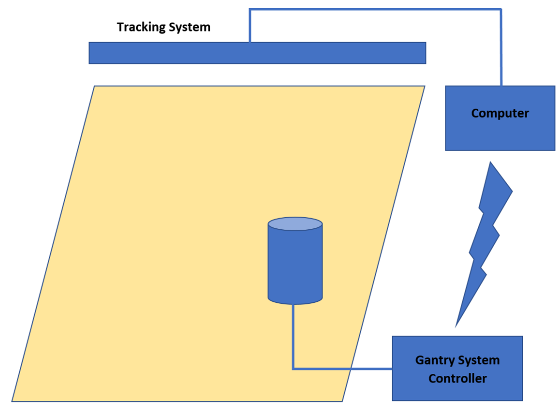

FIGURE 2. Data Acquisition Setup

Data Processing Let's define any tracked position by the pair (x, y) and the preset positions, P_i where $i \in \{1,2,3,4\}$, by (x_i, y_i). The vision tracking system produces a list of position values at a rate of 120 Hz. First, we need to calculate the dwell time at every position P_i during the gantry system movement sequence. We consider the gantry system tool in the position P_i when it is measured to fall in a circle with the center of P_i and a radius of R. The condition is defined as follows

$$\sqrt{(x - x_i)^2 + (y - y_i)^2} \leq R. \tag{1}$$

We set the number of runs at each channel setting to M and the number of cycles per run to N. The dwell times sequence at P_i in the mth run is denoted by $d_i(m)$ which is defined as the vector of the times over which the gantry system tool stayed within a distance R of P_i without interruption. The elements of the dwell times vector are denoted by $d_i(m,n)$ where n is the index of the tool being at the position P_i at each cycle. The average dwell time for each position, denoted by $\bar{d_i}$, is then calculated as follows

$$\bar{d_i} = \frac{1}{MN} \sum_{m=1}^{M} \sum_{n=1}^{N} d_i(m,n). \quad (2)$$

The preset dwell times for various positions are denoted by D_i which equals 2, 1, 0.5, 0.1 seconds, respectively. The average normalized absolute error in the dwell time for P_i, which is denoted by $\tilde{e}_i$, is then expressed as follows

$$\tilde{e}_i = \frac{1}{MN} \sum_{m=1}^{M} \sum_{n=1}^{N} \frac{|d_i(m,n) - D_i|}{D_i}, \quad (3)$$

and the average normalized absolute error in the dwell time over all positions is calculated as follows

$$\tilde{e} = \frac{\tilde{e}_1 + \tilde{e}_2 + \tilde{e}_3 + \tilde{e}_4}{4}. \quad (4)$$

Another performance criterion is the average total run time of the experiment which is denoted by T. The total run time for the mth run is denoted by $T(m)$. The value of $T(m)$ is the period of time since the run starts with the gantry system tool at P_1 and ends after all the N cycles with the gantry system back to P_1. Then, the value of T is calculated as follows

$$T = \sum_{m=1}^{M} T(m) \quad (5)$$

Finally, we also evaluate the number of incomplete runs, denoted by M_I, which is defined as the number of runs at a specific setting where the run has not reached its end due to the wireless network drop.

Numerical Results

In this section, we present the results obtained by running the experiment for various system and channel parameters. We set the distance between the gantry system and the supervisory computer to {20, 25, 30, 35} meters. The shadowing variance takes the values {0, 20, 40, 60} dB. We use three different wireless channel settings over the RF channel emulator, namely, free-space, LOS, and NLOS. Free-space represents the ideal channel with loss exponent of 2 and ideal CIR with no multipath or fading. The LOS and NLOS channel parameters are set according to the measurements in [1]. In the case of LOS, the loss exponent is 1.8 and the CIR taps vary according to a Ricean distribution. In the case of NLOS, the loss exponent is 2.7 and the CIR taps vary according to a Rayleigh distribution.

In this work, we set the number of runs for each setting to $M = 5$. We set the number of cycles per run to $N = 30$. The total run time of the experiment is measured to be around 347 seconds when no communications errors occur and the dwell times at P_1, P_2, P_3, and P_4 are set to 2, 1, 0.5, 0.1 seconds, respectively. The radius R is set to 0.25 millimeter. It is important to note that the Wi-Fi network may be dropped if certain data are missed or delayed which may randomly happen. Also, the effects of missing various types of data are different and hence may cause longer wait times in some cases than the others. In the following subsections, we show the numerical results of various performance criteria and highlight the values which deviate considerably from the typical values.

Total Run Time The typical run time is about 347 seconds, but due to the wireless channel imperfections, the total run time increases when the gantry system tool stops at certain positions longer than required because no new commands are received by the gantry system controller. First, the performance of LOS and NLOS is almost perfect for short distances and low shadowing variance values. The highlighted values are the ones which deviated from the typical value of the system run time. In most practical scenarios, shadowing cannot be more than 20 dB and hence the performance is acceptable for distances up to al-

TABLE 1. Total Run Time in Seconds

Dist.	Shadowing	Free-space	LOS	NLOS
20 m	0 dB	347.0067	347.2533	346.8383
	20 dB	348.0033	347.0633	356.5867
	40 dB	348.2983	353.6729	403.2833
	60 dB	357.2417	427.5389	-
25 m	0 dB	347.2933	346.9800	347.7875
	20 dB	347.3133	346.9708	349.2208
	40 dB	376.0967	354.5563	436.4000
	60 dB	358.0167	375.2278	-
30 m	0 dB	347.3033	347.2567	346.9229
	20 dB	347.675	347.1583	407.6313
	40 dB	348.4861	373.6833	364.9083
	60 dB	361.1958	375.6292	-
35 m	0 dB	347.6233	347.1167	347.6542
	20 db	347.7083	352.6542	377.6104
	40 dB	424.925	375.3983	467.3500
	60 dB	354.2	370.5375	-

most 30 meters. All the runs at NLOS with 60 dB shadowing were not completed.

Average Normalized Error The average normalized error in dwell times represents the average of the normalized deviations of dwell times at all four positions of the gantry systems. In the following subsection the average values of the dwell times are shown. Due to the data acquisition scheme, the typical value of the average normalized error is around 0.26. Depending on the type of dropped packets, the network is dropped or the gantry system tool is stopped at a location for a long time. As a result, the errors are generally higher for poor channels, but may take exceptionally high values at certain settings.

TABLE 2. Average Normalized Error

Dist.	Shadowing	Free-space	LOS	NLOS
20 m	0 dB	0.2660	0.2628	0.2767
	20 dB	0.2665	0.2666	0.3951
	40 dB	0.2721	0.3424	0.4279
	60 dB	0.2641	1.2421	-
25 m	0 dB	0.2665	0.2618	0.2784
	20 dB	0.2628	0.2612	0.6432
	40 dB	0.3728	0.6581	0.9981
	60 dB	0.9803	0.7500	-
30 m	0 dB	0.2643	0.2705	0.2744
	20 dB	0.2593	0.2645	1.3256
	40 dB	0.3436	1.0714	0.5307
	60 dB	0.3937	0.8598	-
35 m	0 dB	0.2636	0.2620	0.2779
	20 dB	0.4979	0.2799	2.1956
	40 dB	0.9447	0.4860	0.6589
	60 dB	0.5029	0.4153	-

Average Dwell Times at Various Positions In this subsection, we present the average dwell times at all four positions of the gantry system. In certain cases where the gantry system tool performs a task which requires controlled timing, the increase of dwell time is considered a major problem in these applications. As a result, the wireless network has to operate within settings that guarantee satisfactory performance.

TABLE 3. Average Dwell Time in Seconds at P_1

Dist.	Shadowing	Free-space	LOS	NLOS
20 m	0 dB	2.0825	2.0805	2.0791
	20 dB	2.0811	2.0808	2.0763
	40 dB	2.0765	2.0685	3.1047
	60 dB	2.0751	2.2285	-
25 m	0 dB	2.0803	2.0809	2.0781
	20 dB	2.0803	2.0807	2.3019
	40 dB	2.9579	2.0780	2.2129
	60 dB	1.9876	2.0876	-
30 m	0 dB	2.0805	2.0801	2.0796
	20 dB	2.0793	2.0795	2.9043
	40 dB	2.0772	2.4617	2.1381
	60 dB	2.0755	2.2027	-
35 m	0 dB	2.0799	2.0784	2.0785
	20 dB	1.8011	2.2293	2.1386
	40 dB	3.5654	2.0776	4.5896
	60 dB	2.0758	2.0759	-

TABLE 4. Average Dwell Time in Seconds at P_2

Dist.	Shadowing	Free-space	LOS	NLOS
20 m	0 dB	1.0793	1.0769	1.0749
	20 dB	1.0783	1.0781	1.0743
	40 dB	1.1027	1.0889	1.0745
	60 dB	1.0763	1.0750	-
25 m	0 dB	1.0784	1.0784	1.0764
	20 dB	1.0787	1.0773	1.0750
	40 dB	1.0773	1.0765	3.4386
	60 dB	1.1220	1.3669	-
30 m	0 dB	1.0781	1.0780	1.0759
	20 dB	1.0768	1.0776	1.0754
	40 dB	1.0759	1.0761	2.0691
	60 dB	1.1293	1.0953	-
35 m	0 dB	1.0774	1.0777	1.0750
	20 dB	1.1994	1.0773	1.0720
	40 dB	1.5324	1.9765	1.0709
	60 dB	1.3594	1.0851	-

TABLE 5. Average Dwell Time in Seconds at P_3

Dist.	Shadowing	Free-space	LOS	NLOS
20 m	0 dB	0.5839	0.5826	0.5838
	20 dB	0.5828	0.5826	0.8248
	40 dB	0.5827	0.7386	0.5832
	60 dB	0.5829	0.5814	-
25 m	0 dB	0.5826	0.5834	0.5846
	20 dB	0.5826	0.5826	1.1497
	40 dB	0.5822	0.7936	0.8091
	60 dB	0.6009	0.5819	-
30 m	0 dB	0.5824	0.5953	0.5851
	20 dB	0.5825	0.5829	1.3481
	40 dB	0.5814	0.5824	0.5823
	60 dB	0.6525	0.5902	-
35 m	0 dB	0.5807	0.5843	0.5842
	20 dB	0.6486	0.5841	0.6347
	40 dB	0.5810	0.5833	0.7065
	60 dB	0.9295	0.8857	-

TABLE 6. Average Dwell Time in Seconds at P_4

Dist.	Shadowing	Free-space	LOS	NLOS
20 m	0 dB	0.1776	0.1769	0.1825
	20 dB	0.1782	0.1783	0.1818
	40 dB	0.1782	0.1769	0.1918
	60 dB	0.1777	0.5616	-
25 m	0 dB	0.1782	0.1761	0.1829
	20 dB	0.1767	0.1762	0.2047
	40 dB	0.1771	0.2930	0.1829
	60 dB	0.4591	0.3426	-
30 m	0 dB	0.1774	0.1774	0.1812
	20 dB	0.1756	0.1775	0.4079
	40 dB	0.2097	0.4814	0.1820
	60 dB	0.2103	0.4062	-
35 m	0 dB	0.1776	0.1763	0.1829
	20 dB	0.2396	0.1759	0.9372
	40 dB	0.3302	0.1762	0.1857
	60 dB	0.1755	0.1767	-

Incomplete Runs Finally, we present the number of incomplete runs out of five for each of the settings. The network drop is not related to the period of communication link interruption, but it is related to the type of packets dropped. However, having higher shadowing variance is a main cause of dropping the network connectivity compared to the channel distance and CIR characteristics.

TABLE 7. The Number of Incomplete Runs at Each Setting

Dist.	Shadowing	Free-space	LOS	NLOS
20 m	0 dB	0	0	0
	20 dB	0	0	0
	40 dB	0	1	2
	60 dB	3	2	5
25 m	0 dB	0	0	1
	20 dB	0	1	3
	40 dB	0	1	0
	60 dB	3	2	5
30 m	0 dB	0	0	1
	20 dB	1	0	1
	40 dB	2	1	2
	60 dB	3	3	5
35 m	0 dB	0	1	1
	20 dB	1	1	1
	40 dB	3	0	4
	60 dB	2	3	5

Conclusions

In this paper, we introduced an experimental study of the impacts of wireless channel parameters on a gantry system performance. We introduced the testbed architecture, the experiment setup, and performance measurements. We deployed a vision tracking system for collecting position data from the gantry system. We have shown that the main wireless impact on the performance is longer dwell times at certain positions of the gantry system tool path. The used gantry system has a G-code commands buffer which reduced the abrupt variations on the performance. The system performance is clearly different for LOS and NLOS settings. Generally, wireless technology benefits can be reaped on similar systems by designing the system appropriately based on the RF environment of the gantry system. Design parameters include buffer size, maximum transmission range, and requirements on LOS existence.

ACKNOWLEDGMENT

We would like to thank Rushad Antia for his efforts in building the testbed and setting up the supervisory computer.

Disclaimer

Certain commercial equipment, instruments, or materials are identified in this paper in order to specify the experimental procedure adequately. Such identification is not intended to imply recommendation or endorsement by the National Institute of Standards and Technology, nor is it intended to imply that the materials or equipment identified are necessarily the best available for the purpose.

REFERENCES

[1] Candell, R., Remley, C., Quimby, J., Novotny, D., Curtin, A., Papazian, P., Koepke, G., Diener, J., and Kashef, M., 2017. Industrial wireless systems: Radio propagation measurements. Tech. rep., National Institute of Standards and Technology, Gaithersburg, MD.

[2] Nixon, M., 2012. A comparison of wirelesshart and isa100.11a. Tech. rep., MSU-CSE-06-2; Emerson Process Management, Round Rock, TX, USA.

[3] Bregulla, M., Feucht, W., Koch, J., de Mur, G., Schade, M., Weczerek, J., and Wenzel, J., 2011. Wireless solutions in automation. ZWEI, March.

[4] Wireless control of gantry cranes in industries. EMNICS Technologies Pvt Ltd, 2015.

[5] Gaspar, T., Ridge, B., Bevec, R., Bem, M., Kova, I., Ude, A., and Gosar, Z. "Rapid hardware and software reconfiguration in a robotic workcell". In 2017 18th International Conference on Advanced Robotics (ICAR), pp. 229–236.

[6] Al-Saedi, I. R. K., Mohammed, F. M., and Obayes, S. S., 2017. "CNC machine based on embedded wireless and internet of things for workshop development". In 2017 International Conference on Control, Automation and Diagnosis (ICCAD), pp. 439–444.

[7] Wozniak, A., and Jankowski, M., 2016. "Wireless communication influence on CNC machine tool probe metrological parameters". *The International Journal of Advanced Manufacturing Technology,* ***82***(1), Jan, pp. 535–542.

[8] Kulkarni, A. D., Sujatha, K., and Shinde, N., 2015. "Article: A pick and place robot: A flexible robot with adjustable rubber hand". *International Journal of Computer Applications,* ***128***(8), October, pp. 16–19. Published by Foundation of Computer Science (FCS), NY, USA.

[9] X-carve [online]. https://www.inventables.com/technologies/x-carve. Accessed: 08/10/2018.

[10] Smid, P., 2008. *CNC Programming Handbook*. 3rd Edition, ISBN 9780831133474.

[11] Industrial Intel Bay Trail Fanless NUC computer ML100G-10. https://www.logicsupply.com/ml100g-10/. Accessed: 2018-08-13.

[12] Antaira stw-611c: Product specifications. http://www.antaira.com/products/STW-611C. Accessed: 2018-08-13.

[13] Rfnest: product specifications. http://www.i-a-i.com/wp-content/uploads/2017/07/RFnest-Specsheet-2017.pdf. Accessed: 2017-08-14.